EFFECT OF DIFFERENT COMPACTION PRESSURES ON PHYSICOMECHANICAL PROPERTIES OF AKERMANITE BIOCERAMICS USING CALCIUM DERIVED FROM DENTAL MOULD WASTE

Nur Liyana Mohd Rosli^{1,2} and Yanny Marliana Baba Ismail^{1,*}

¹ Biomaterials Niche Group, School of Materials and Mineral Resources Engineering,
 Engineering Campus, Universiti Sains Malaysia, 14300 Nibong Tebal, Penang, Malaysia.
 ²Advance Material Processing & Design, Faculty of Mechanical Engineering Technology,
 Universiti Malaysia Perlis, Kampus Pauh Putra, 02600 Arau, Perlis, Malaysia.

*yannymarliana@usm.my

Abstract. This study aimed to produce akermanite bioceramics derived from dental mould waste (DMW) via high-energy planetary ball milling followed by subsequent sintering. Alkaline roasting and caustic leaching were utilised to extract calcium from dental mould waste prior to synthesise akermanite. Uniaxial pressing was used to prepare the green compacts with different compacting pressures of 200 and 250 MPa. The pellets were sintered in a chamber furnace at 1225 °C for three hours with a constant heating and cooling rate of 5 °C/min. The effects of compaction pressure on the physical and mechanical properties of the sintered akermanite were investigated. X-ray diffraction (XRD) analysis revealed that the major phase of these sintered samples is crystalline akermanite, with diopside as a minor phase. The microstructural analysis of the fractured surfaces for the sintered akermanite bioceramics exhibited a transgranular fracture mode, indicating the presence of strong grain boundaries and leading to high mechanical strength. Considering the quality of the pellet and slightly higher DTS value, 200 MPa was selected as the preferable compaction pressure rather than 250 MPa. At this condition, the sintered akermanite possesses a diametral tensile strength of 5.25 ± 0.53 MPa, which falls in the range of the human cancellous bone (2-12) MPa), while higher 250 MPa, the diametral tensile strength was 5.18 ± 0.31 MPa.

Keywords: Dental mould waste (DMW), calcium sulphate dihydrate, chromium removal, alkaline roasting, caustic leaching

Article Info

Received 19th January 2023 Accepted 5th April 2023 Published 1st May 2023

Copyright Malaysian Journal of Microscopy (2023). All rights reserved.

ISSN: 1823-7010, eISSN: 2600-7444

Introduction

In recent years, calcium magnesium silicate-based, CaO-MgO- SiO₂, bioceramics have appeared as an alternative bioceramics to the well-known calcium phosphate (CaP)-based family, like the hydroxyapatite (HA) and β-tricalcium phosphate (β-TCP). The main drawbacks of CaP-based bioceramics are poor compressive strength and low fracture toughness [1], slow degradation kinetics [2], weak bone-bonding ability [3] and lack of osteoinductivity [4]. Hence, CaO-MgO-SiO₂ ceramics have recently been preferred over the phosphate groups owing to their controllable degradation rate and adequate mechanical properties in maintaining mechanical support during bone tissue formation [5]. The unique characteristics of these bioceramics make them suitable candidates for future bone substitute materials. Ideally, a bone substitute material should possess similar mechanical behaviour as the native bone tissue to be substituted in preventing post-operative effects, offers an affordable synthesis cost and biocompatible with the surrounding tissue, which facilitates new bone formation [6].

Akermanite, Akr (Ca2MgSi2O7), a calcium magnesium silicate-based bioceramics, demonstrated a high potential in treating bone defects. Calcium, magnesium and silicon play vital roles in forming bone minerals, assisting in biomineralisation and bone growth metabolism [7]. Compared to tricalcium phosphate (TCP), akermanite has greater mechanical properties and promotes better osteogenesis and biodegradation, which lead to rapid bone formation [8]. Interestingly, CaO-MgO-SiO2 systems are subjected to highly flexible design capability by tailoring their structural and chemical composition to comply with the clinical requirements. Several techniques in synthesising akermanite have been reported, including the solid-state reaction [9], sol-gel [10] and solution combustion method [11]. In most chemical syntheses, commercial-grade calcium, magnesium and silicon sources were used in preparing the akermanite ceramics. Recently, our group has successfully synthesised akermanite using cockleshell, dolomite and rice husk ash biowastes [12]. This has motivated us to find other sources of biowastes, particularly calcium-rich biowaste, as calcium is the main precursor in making akermanite bioceramics.

Dental mould waste (DMW) consisting of calcium sulphate dihydrate (CaSO₄.2H₂O) has been identified as a potential calcium-rich biowaste. Dental mould waste is made of gypsum and known as type 3 dental stone, which has been classified by American Dental Association (ADA). There are five different types of gypsum products with specific properties to meet clinical dentistry requirement. DMW is one of the most abundant biowastes produced by dental clinics, institutes or laboratories in Malaysia, as dental moulds are patient-specific, i.e., one patient per mould. This biowaste is typically discarded as municipal solid waste and being dumped in landfills, as it is considered as zero-value material. Irresponsible disposal of this waste could lead to health issues, and environmental pollution as DMW could react with the soil and subsequently emit an unpleasant odour similar to that of rotten eggs [13]. In reality, the nature of calcium sulphate dihydrate being an anaerobic in a humid environment. Due to the fact that this DMW also includes trace levels of chromium, the leaching of this trace element could impair soil quality and render it poisonous. With the growing environmental concerns, reducing this waste by converting the zero-value DMW into functional bioceramics is crucial. This sustainable approach may also educate society to recycle and reuse waste, reduce environmental pollution, and indirectly provide cheaper bioceramics products to help needy patients.

In this study, the sintered akermanite bioceramics were produced by compacting the powder at different pressures of 200 and 250 MPa, followed by sintering at 1225 °C. Most of the previous studies reported on the physical, mechanical and biological properties of akermanite ceramics correspond to the sintering behaviour [14]. To date, no studies have demonstrated the impact on compaction pressures on the properties of akermanite bioceramics derived from dental mould waste. This study investigates the effect of different compaction pressures on the physicomechanical properties of akermanite bioceramics. All the sintered samples were then characterised for their phase formation, chemical bonding, densification, mechanical strength and morphologies to select the most suitable pressure in preparing akermanite bioceramics.

Materials and Methods

Calcium Source Extraction

Type 3 green dental mould waste (DMW) was collected from Advanced Medical and Dental Institute (AMDI), Universiti Sains Malaysia (USM) located at Kepala Batas, Penang. The refinement of calcium source derived from DMW has been reported in our previous work [15]. Basically, the green dental mould wastes were cleaned, crushed, and ground into finer powders using a high-energy planetary ball mill (RETSCH Models PM 100). The crushed DMW was milled for an hour at 300 rpm speed with a 2:1 ball-to-powder ratio and 4:1 water-to-powder ratio. The as-milled DMW powder was mixed with 2:1 ratio of Na₂CO₃ (Merck, 99.50% pure)-to-Cr₂O₃ before roasting. The mixed powders were filled into an alumina crucible and heated to 1000 °C for an hour with a heating rate of 5 °C/min. The Na₂CO₃ reacts with Cr₂O₃ present in the CaSO₄.2H₂O during roasting and transforms it into soluble Na₂CrO₄, which will ease the extraction of chromium during the leaching process. Roasting is a process of heating. In this process, the extraction of chromium is achieved by heating the mineral (in this case, CaSO₄.2H₂O containing Cr₂O₃) with alkali salts (Na₂CO₃). The sample was roasted at 1000 °C as Cr₂O₃ began to react with Na₂CO₃, producing Na₂CrO₄ at 1000 °C [16]. The roasted powders were then caustic leached with 7M NaOH (Merck, 99.00% pure) for another hour. NaOH acts as a leaching medium that enables the separation of chromium by removing the soluble Na₂CrO₄ through the filtrate. The solution was directly vacuum filtered through a Whatman filter paper using a Buchner filter. At the same time, the residue and the concentrated NaOH solution can be simultaneously reacted, resulting in a white precipitate Ca(OH)₂ obtained after the filtration process. The solid residue was rinsed five times with deionised water. The filtered cake was then dried in an oven at 100 °C for 24 hours. The dried cake was eventually ground to powder using an agate mortar and pestle, forming Ca(OH)₂ powders.

Sample Preparation

High-energy planetary ball milling was again used to prepare akermanite bioceramics powders. The obtained Ca(OH)₂ powders were milled and mixed together with the commercial-grade silicon dioxide (Sigma Aldrich, 99.9% SiO₂) and magnesium oxide (Sigma Aldrich, 98% MgO) with a stoichiometric ratio of Ca: Mg: Si (2: 1: 2). A 10:1 of balls to powder and 4:1 water to powder ratios were prepared and then placed in a zirconia vial. In this work, wet milling using deionised water was utilised to mix the precursors mechanically. The mixing was performed for four hours with a rotational speed of 500 rpm using the PM 100 planetary mill. The as-milled mixture was oven dried at 100 °C for 24 hours and then

ground with agate mortar and pestle. To prepare the green compact, 0.5 g of the produced akermanite powders were firstly weighed and carefully placed in a 13 mm diameter stainless steel die. The powders were then uniaxially compacted at 200 or 250 MPa with two minutes holding time. The green compacts were then kept for 24 hours in a desiccator. Sintering was then conducted at 1225 °C for three hours with 5 °C/min heating and cooling rate using a chamber furnace (Lenton, UK).

Material Characterisations

Phase analysis was carried out on sintered akermanite samples using X-Ray Diffraction analysis (XRD; Bruker D2 Phaser XRD, Germany). Cu-K α radiation was set at λ = 1.5418 Å with diffraction angles 2θ of $10^{\circ} \le 2\theta \le 80^{\circ}$. Rietveld refinement of XRD patterns was analysed using PANalytical X'pert Highscore software based on ICDD database references. Fourier Transform Infrared (FTIR) spectroscopy was used to determine the functional groups of akermanite samples. The spectrum was recorded using Perkin Elmer at 400 - 4000 cm⁻¹ under a transmittance mode (%T). Sintered samples were sputter-coated with a thin platinum layer to facilitate in morphological observations using Field Emission Scanning Electron Microscopy (FESEM; Zeiss SupraTM Gemini 35 VP).

Relative density and open porosity were measured according to the ASTM B 962-17 Standard: Standard Test Methods for Density of Compacted or Sintered Powder Metallurgy (PM) by employing Archimedes' principle. Vickers microhardness and fracture toughness tests were performed on polished sintered akermanite using Leco LM248AT Microhardness tester with test load of 2 kg-force (kg.f) in compliance with the ASTM E 384–99 Standard: Standard Test Method for Microindentation Hardness of Materials. Fracture toughness was determined based on the radial crack length measured from the centre point of the indented area and ($K_{\rm IC}$) was calculated using the following Equation 1;

$$K_{\rm IC} = 0.0824 \frac{F}{C^{\frac{3}{2}}} \tag{1}$$

where, F is the applied load (N), and C is radial crack length (m) measured from the center point of the indented area.

Diametral Tensile Strength (DTS) test was carried out on the sintered ceramics with 0.5 mm/min loading using the universal testing machine (INSTRON 3367) following the ASTM D3967–95a Standard: Standard Test Method for Splitting Tensile Strength of Intact Rock Core Specimens. Three sintered samples (n=3) were used for each characterisation performed.

Results and Discussion

Physicochemical Analysis

The XRD patterns of the samples prepared with 200 and 250 MPa uniaxial pressing are shown in Figure 1. Almost all the detected peaks matched well with the akermanite (Ca₂MgSi₂O₇, ICDD data: 01-079-2425), while the remnant peaks belong to diopside (ICDD data: 04-011-6812) as the minor phase. Diopside is compositionally similar to akermanite with the chemical formula of CaMgSi₂O₆. Akermanite has a tetragonal crystal structure with

the lattice parameters of $a = b \neq c$ and $\alpha = \beta = \gamma = 90^{\circ}$. This structure belongs to a space group of P-421m with Z = 2. Based on the diffraction pattern obtained, it clearly showed that changing compaction pressure has no significant effect on the phase formation.

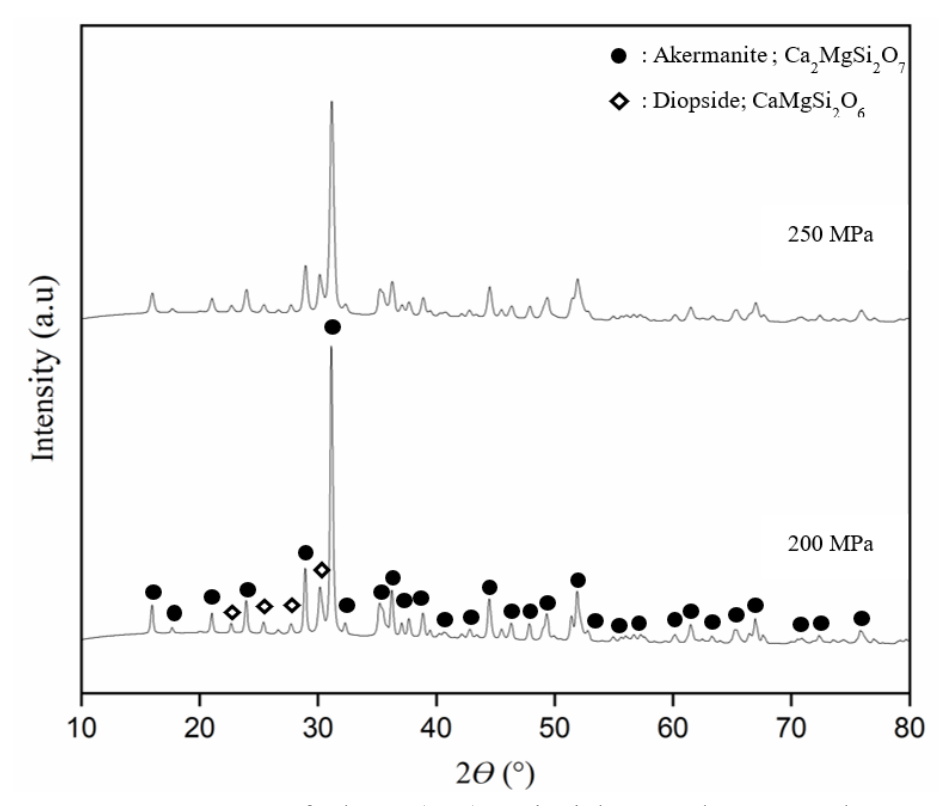


Figure 1: XRD patterns of Akr-Ca(OH)₂ uniaxial pressed at 200 and 250 MPa

Phase analysis was performed using Rietveld refinement. Both samples demonstrated evidence of a main peak of single phase akermanite in the ranges of 31° - 32° . The high intensity and sharp peaks corresponding to (h k l) indices at (111), (201), (211), (310), (212), and (312) with peak angles originated at $2\theta \approx 23.9^{\circ}$, 28.9° , 31.1° , 36.2° , 44.4° and 51.9° . The lattice parameter 'a', as well as the unit cell volume, showed a decrease with increasing compaction pressure, as shown from the data given in Table 1. The unit cell volume resulting from ($V_{cell} = a^2 \times c$). These data reveal that the compaction pressure has an effect on lattice parameters while the crystalline structure remains unchangeable.

Table 1: Crystallographic data of sintered akermanite with different compaction pressures

Sample	Crystal system	$A = \beta = \gamma$ (deg)	a = b (Å)	c (Å)	V _{cell} (Å ³)
Akr-Ca(OH) ₂ -200	Tetragonal	90	7.833	5.008	307.428
Akr-Ca(OH) ₂ -250	Tetragonal	90	7.827	5.008	306.815

The FTIR spectra of the sintered samples illustrated in Figure 2 showed the typical bands of the akermanite bioceramics [5]. A peak belongs to the bending modes of O–Ca–O was detected at 404 cm⁻¹. The observed bending modes of O–Mg–O were noticed at 475 cm⁻¹ and 505 cm⁻¹, respectively. The band at 587 cm⁻¹ was assigned to the Ca=O group. The dual peaks at 642 and 683 cm⁻¹ were attributed to the absorption bands of O–Si–O. The

stretching modes of Si–O was located at 852, 936, and 975 cm⁻¹, while symmetric stretching vibration of Si–O–Si is observed at 1011 cm⁻¹ [9]. The moisture adsorption at 3468 cm⁻¹ was attributed to the OH– group.

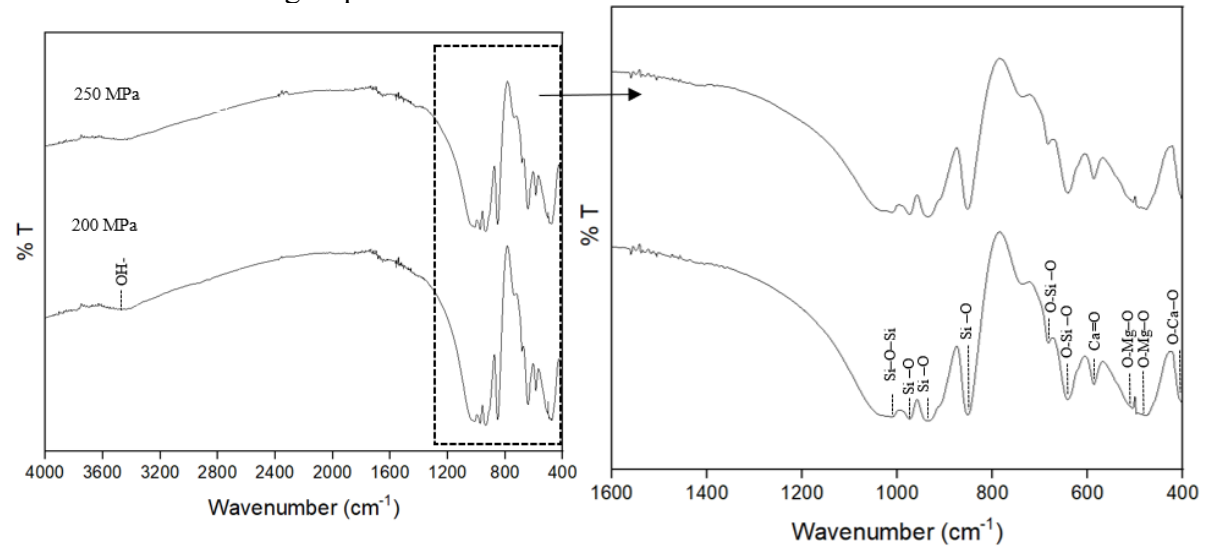


Figure 2: FTIR spectrums of Akr-Ca(OH)₂ uniaxial pressed at 200 MPa and 250 MPa

Physical Properties

In this study, relative density and open porosity of the sintered samples calculated as a function of compaction pressure, are presented in Table 2. The relative density of the sintered samples increased slightly from $57.74 \pm 2.23\%$ to $58.18 \pm 0.47\%$ by increasing compaction pressure from 200 to 250 MPa. Concurrently, the percentage of open porosity showed a small reduction $46.96 \pm 2.13\%$ to $45.07 \pm 1.55\%$ with the increment in the compaction pressure. This could be due to the rearranging of the particles during compaction under higher pressure, which resulted in reducing pores between the particles. Upon sintering, the closely packed particles react more effectively as there are fewer pores between them, resulting in better densification.

Table 2: Relative density and open porosity of sintered akermanite with different compaction pressures

Sample	Relative density (%)	Open porosity (%)
Akr-Ca(OH) ₂ -200	57.74 ± 2.23	46.96 ± 2.13
Akr-Ca(OH) ₂ -250	58.18 ± 0.47	45.07 ± 1.55

Mechanical Properties

Vickers microhardness (Hv), fracture toughness (K_{IC}) and diametral tensile strength (DTS) of sintered akermanite with different compaction pressures are summarised in Table 3. The microhardness value reached the highest value of 0.42 ± 0.01 GPa at 250 MPa. The calculated fracture toughness (K_{IC}) value indicated a similar trend to hardness. The K_{IC} value

obtained at 200 MPa is 0.27 ± 0.04 MPa.m^{1/2}, and by increasing further 50 MPa compaction pressure, the $K_{\rm IC}$ value increased about 3-folds (0.62 \pm 0.01 MPa.m^{1/2}). It has been reported that human cancellous bone has a fracture toughness of 0.10–0.80 MPa.m^{1/2}. [17]. Thus, both $K_{\rm IC}$ values obtained reliable in the range.

The DTS values of Akr-Ca(OH)₂ resulting from compaction pressure of 200 and 250 MPa were 5.25 ± 0.53 MPa and 5.18 ± 0.31 MPa, respectively. A slight decrease in DTS values was observed with increasing compaction pressure from 200 MPa to 250 MPa. This could be due to the springback effect, which increased with compaction pressure, particularly with fine powder and no plasticiser.

Table 3: Mechanical properties of sintered akermanite with different compaction pressures

Sample	$H_{\rm V} \pm { m SD}$	$K_{\rm IC} \pm { m SD}$	$DTS \pm SD$
-	(GPa)	$(MPa.m^{1/2})$	(MPa)

Akr-Ca(OH)₂ -200 0.14 ± 0.01 0.27 ± 0.04 5.25 ± 0.53 0.42 ± 0.01 0.62 ± 0.01 5.18 ± 0.31 Akr-Ca(OH)2 -250

Moreover, it was also observed that some of the Akr-Ca(OH)2 pellets compacted at 250 MPa show characteristics of end capping rather than the smooth pellet during the compaction process, as can be seen in Figure 3. The end capping develops as a result of the elastic springback's constraint upon release of the punch pressure [18]. It might have happened when the green bodies were being ejected from the die, and the capping was generated as the particles cannot relieve the stress caused by pressing and ejection. This type of defect cannot be healed by sintering and thus affects the DTS measurement as this technique is very sensitive to the presence of flaws. Regardless of the compaction pressure applied, the resultant strength values achieved for both samples fall within the range of human cancellous bone (2–12 MPa) [19].



Figure 3: Observation of green compact pellet with end capping, uniaxially pressed under 250 MPa

Microstructural Analysis

Figure 4 shows the morphological observation of the sintered samples subjected to different compaction pressures observed under FESEM. Furthermore, a transgranular fracture mechanism was visible in both sintered samples. This fracture mode contributes greatly to strengthening the grain boundaries and also resistance to crack propagation [20]. The microstructures clearly indicated almost similar pore populations amongst the agglomerates for both samples uniaxially pressed under 200 and 250 MPa. It can be observed that sintered samples were highly porous, which thus influenced the low values of the mechanical properties, as discussed earlier.

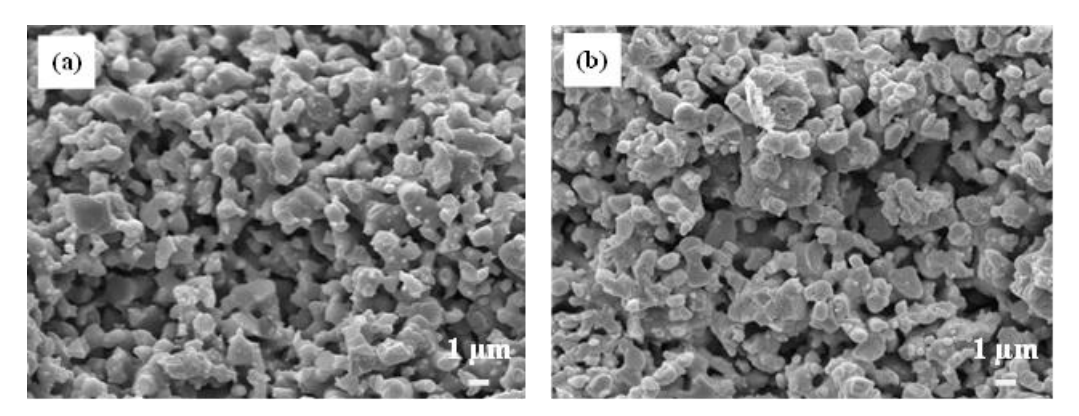


Figure 4: FESEM micrographs at compaction pressures of (a) 200 MPa and (b) 250 MPa fractured surface of the sintered akermanite

Conclusions

The akermanite bioceramics using calcium derived DMW waste have been synthesised via high-energy planetary ball milling followed by sintering at 1225 °C. Compaction pressure has a minor impact on the sintered akermanite bioceramics, in which slightly denser and harder akermanite are produced by uniaxially pressed at 250 MPa. No notable changes are shown in the phase formation and chemical bonding. The use of dental mould waste to fabricate akermanite could promote effective waste management, reduce environmental pollution, and provide a cheaper source of future bone substitutes for patients.

Acknowledgements

The financial support for this research was provided by Universiti Sains Malaysia Research University Grant (RUI): 1001/PBAHAN/8014143.

Author Contributions

All authors contributed toward data analysis, drafting and critically revising the paper and agree to be accountable for all aspects of the work.

Disclosure of Conflict of Interest

The authors have no disclosures to declare.

Compliance with Ethical Standards

The work is compliant with ethical standards.

References

- [1] Wei, S., Ma, J. X., Xu, L., Gu, X. S. & Ma, X. L. (2020). Biodegradable materials for bone defect repair. *Military Medical Research*, 7(1), 1–25.
- [2] Wu, C. & Chang, J. (2013). A review of bioactive silicate ceramics. *Biomedical Material*, 8(3), 032001.
- [3] Bulut, B. & Duman, S. (2022). Evaluation of mechanical behavior, bioactivity, and cytotoxicity of chitosan/akermanite-TiO₂ 3D-printed scaffolds for bone tissue applications. *Ceramic International*, 48, 21378–21388.
- [4] Cheng, L., Ye, F., Yang, R., Lu, X., Shi, Y.,Li, L., Fan, H. & Bu, H. (2010). Osteoinduction of hydroxyapatite β -tricalcium phosphate bioceramics in mice with a fractured fibula. *Acta Biomaterialia*, 6, 1569–1574.
- [5] Sharafabadi, A. K., Abdellahi, M., Kazemi, A., Khandan, A. & Ozada, N. (2017). A novel and economical route for synthesizing akermanite (Ca₂MgSi₂O₇) nano-bioceramic. *Materials Science and Engineering C*, 71, 1072–1078.
- [6] Putra, N. E., Borg, K. G. N., Diaz-Payno, P. J., Leeflang, M. A., Klimopoulou, M., Taheri, P., Mol, J. M. C., Fratila-Apachitei, L. E., Huan, Z., Chang, J., Zhou, J. & Zadpoor, A. A. (2022). Additive manufacturing of bioactive and biodegradable porous iron-akermanite composites for bone regeneration. *Acta Biomaterialia*, 148, 355–373.
- [7] Tavangarian, F., Zolko, C. A., Fahami, A., Forghani, A. & Hayes, D. (2019). Facile synthesis and structural insight of nanostructure akermanite powder. *Ceramics International*, 45(6), 7871–7877.
- [8] Srinath, P., Abdul Azeem, P. & Venugopal Reddy, K. (2020). Review on calcium silicate-based bioceramics in bone tissue engineering. *International Journal of Applied Ceramic Technology*, 17(5), 2450–2464.
- [9] Myat-Htun, M., Mohd Noor, A. F., Kawashita, M. & Baba Ismail, Y. M. (2020). Enhanced sinterability and in vitro bioactivity of barium-doped akermanite ceramic. *Ceramics International*, 46(11), 19062–19068.
- [10] Yuan, X., Wu, T., Lu, T., He, F., Chen, P., Ma, N. & Ye, J. (2022). Enhancement in the osteogenesis and angiogenesis of calcium phosphate cement by incorporating magnesium-containing silicates. *Ceramics International*, 48(15), 1–13.
- [11] Collin, M. S., Venkatraman, S. K., Sriramulu, M., Shanmugam, S., Drweesh, E. A., Elnagar, M. M., Mosa, E. S. & Sasikumar, S. (2021). Solution combustion synthesis of functional diopside, akermanite, and merwinite bioceramics: Excellent biomineralization, mechanical strength, and antibacterial ability. *Materials Today Communications*, 27, 102365.

- [12] Mohammadi, H., Hei, B. Z., Baba Ismail, Y. M., Shariff, K. A. & Mohd Noor, A. F. (2020). Green synthesis of calcium magnesium silicate (Cms-akermanite) using natural biowastes by solid-state sintering route. *Malaysian Journal of Microscopy*, 16(2), 66–76.
- [13] Asabe, R. & Bhansali, M. (2020). Recycling and Reuse of Dental Materials: A Overview. *Journal of Emerging Technologies and Innovative Research*, 7(8), 186–190.
- [14] Han, Z., Feng, P., Gao, C., Shen, Y., Shuai, C. & Peng, S. (2014). Microstructure, mechanical properties and in vitro bioactivity of akermanite scaffolds fabricated by laser sintering. *Bio-Medical Materials and Engineering*, 24(6), 2073–2080.
- [15] Mohd Rosli, N. L. & Baba Ismail, Y. M. (2022). Different Concentrations of Sodium Hydroxide Caustic Leaching of Cr⁶⁺ for Refinement of Calcium Source from Dental Mould Waste. *Malaysian Journal of Microscopy*, 18(1), 46–56.
- [16] Fang, H. X., Li, H. Y. & Xie., B. (2012) Effective chromium extraction from chromium-containing vanadium slag by sodium roasting and water leaching. *The Iron and Steel Institute of Japan International*, 52(11), 1958–1965.
- [17] Gao, C., Peng, S., Feng, P. & Shuai, C. (2017). Bone biomaterials and interactions with stem cells. *Bone Research*, 5, 51–33.
- [18] Niesz, D. E. (1996). A Review of Ceramic Powder Compaction. *Kona Powder and Particle Journal*, 4(3), 44–51.
- [19] Baino, F., Novajra, G. & Vitale-Brovarone, C. (2015). Bioceramics and scaffolds: A winning combination for tissue engineering. *Frontiers in Bioengineering and Biotechnology*, 3, 1–17.
- [20] Feng, P., Gao, C., Shuai, C. & Peng, S. (2015). Toughening and strengthening mechanisms of porous akermanite scaffolds reinforced with nano-titania. *Royal Society of Chemistry Advances*, 5(5), 3498–3507.